

SI Tables and Figures**Spinor Dynamics in Pristine and Mn²⁺ Doped CsPbBr₃ NC: Role of Spin-Orbit Coupling in Ground and Excited State Dynamics**

Aaron Forde¹, Talgat Inerbaev^{2,3}, Dmitri Kilin^{4*}

¹ *Department of Materials Science and Nanotechnology, North Dakota State University, Fargo, North Dakota 58102, United States*

² *L. N. Gumilyov Eurasian National University, Astana, Kazakhstan*

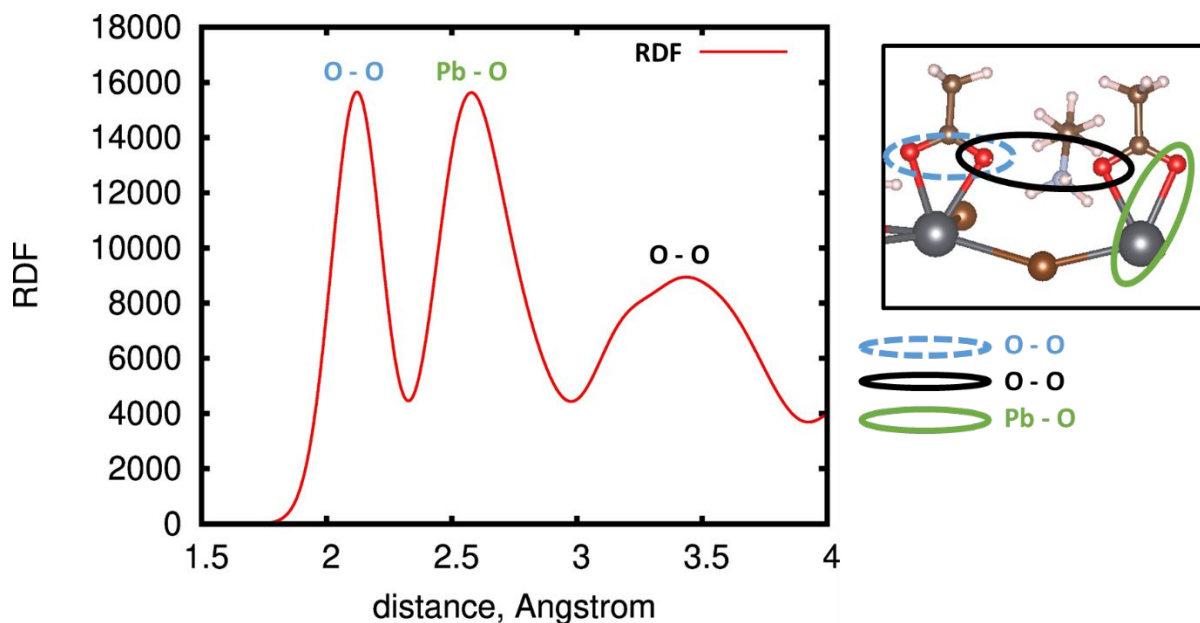
³ *National University of Science and Technology MISIS, 4 Leninskiy pr., Moscow 119049, Russian Federation*

⁴ *Department of Chemistry and Biochemistry, North Dakota State University, Fargo, North Dakota 58102, United States*

*Corresponding Author: dmitri.kilin@ndsu.edu

	<i>Pristine QD Spin-Restricted</i>			<i>Pristine QD Spinor</i>		
	Br 4p	Pb 6s	Pb 6p	Br 4p	Pb 6s	Pb 6p
HO-9	0.65	0.16	0.01	0.53	0.22	0.01
HO-8	0.56	0.18	0.01	0.53	0.22	0.01
HO-7	0.60	0.20	0.01	0.57	0.22	0.01
HO-6	0.61	0.20	0.01	0.57	0.22	0.01
HO-5	0.56	0.21	0.01	0.55	0.21	0.01
HO-4	0.56	0.22	0.02	0.55	0.21	0.01
HO-3	0.52	0.21	0.01	0.55	0.21	0.01
HO-2	0.54	0.22	0.01	0.55	0.21	0.01
HO-1	0.52	0.21	0.01	0.60	0.25	0.02
HO-0	0.59	0.26	0.01	0.60	0.25	0.02
LU+0	0.05	0.01	0.80	0.04	0.00	0.84
LU+1	0.03	0.00	0.78	0.04	0.00	0.84
LU+2	0.05	0.01	0.80	0.04	0.00	0.84
LU+3	0.04	0.01	0.79	0.04	0.00	0.84
LU+4	0.04	0.00	0.79	0.05	0.00	0.82
LU+5	0.04	0.00	0.80	0.05	0.00	0.82
LU+6	0.06	0.00	0.77	0.05	0.01	0.83
LU+7	0.04	0.00	0.70	0.05	0.01	0.83
LU+8	0.03	0.00	0.75	0.07	0.00	0.83
LU+9	0.02	0.01	0.79	0.07	0.00	0.83

SI Table S1: *pDOS of KSO/SKSOs near HOMO-LUMO gap for the pristine QD. For both SR and NCS SOC calculations the valence band edge is composed of Br 4p and Pb 6s states and the conduction band edge is composed of Pb 6p states. Shaded regions represent KSO densities that provide >10%.*



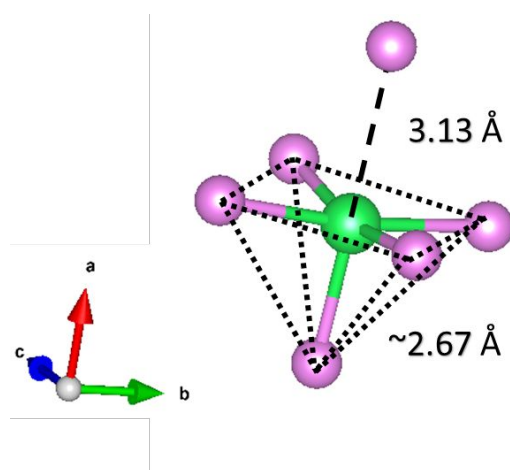
SI Figure S1: $RDF(r,t=0)$ of the ground-state geometry optimized pristine QD considering only Pb-O atoms. We use this method as a way to determine average bond distance between surface Pb^{2+} atoms and AC passivation ligands. To the right of the RDF illustrates the peaks from RDF. The first peak corresponds to average distance between resonant O atoms from the same AC ligand (blue, dashed).. The second peak corresponds to average Pb-O bond distance (green, solid). The broad third peak corresponds to distances between O atoms on different AC ligands (black, solid).

Pristine NC: SKSO Energy and Magnetization						Doped NC: SKSO Energy and Magnetization					
	eV	Mx	My	Mz	M		eV	Mx	My	Mz	M
HO-10	-3.219	0.04	0.22	-0.28	0.36	HO-10	-3.232	-0.178	0.278	-0.045	0.333
HO-9	-3.212	-0.47	-0.23	0.06	0.52	HO-9	-3.221	-0.212	0.056	0.236	0.322
HO-8	-3.212	0.47	0.23	-0.06	0.52	HO-8	-3.214	0.388	0.121	-0.119	0.423
HO-7	-3.190	0.41	0.22	-0.07	0.47	HO-7	-3.207	-0.285	-0.073	0.117	0.317
HO-6	-3.190	-0.41	-0.22	0.07	0.47	HO-6	-3.199	-0.180	-0.074	-0.052	0.201
HO-5	-3.173	0.22	0.06	0.41	0.46	HO-5	-3.192	0.447	-0.301	-0.079	0.545
HO-4	-3.173	-0.22	-0.06	-0.41	0.46	HO-4	-3.189	-0.174	0.254	-0.185	0.359
HO-3	-3.092	0.61	0.12	0.05	0.62	HO-3	-3.091	0.045	0.091	0.591	0.600
HO-2	-3.092	-0.61	-0.12	-0.05	0.62	HO-2	-3.083	-0.047	-0.083	-0.593	0.601
HO-1	-2.937	0.59	-0.09	0.21	0.63	HO-1	-2.800	-0.008	0.001	0.722	0.722
HO-0	-2.937	-0.59	0.09	-0.21	0.63	HO-0	-2.325	0.000	-0.001	0.752	0.752
LU+0	-0.537	0.07	-0.18	0.09	0.21	LU+0	-0.5627	0.064	-0.165	0.066	0.189
LU+1	-0.537	-0.07	0.18	-0.09	0.21	LU+1	-0.5577	-0.063	0.167	-0.069	0.191
LU+2	-0.340	0.05	-0.13	0.03	0.14	LU+2	-0.423	0.077	0.092	-0.126	0.174
LU+3	-0.340	-0.05	0.13	-0.03	0.14	LU+3	-0.4059	-0.100	-0.070	0.085	0.149
LU+4	-0.266	-0.09	0.07	-0.06	0.13	LU+4	-0.3687	0.037	-0.013	-0.109	0.116
LU+5	-0.266	0.09	-0.07	0.06	0.13	LU+5	-0.3587	0.003	-0.062	0.027	0.068
LU+6	-0.238	-0.12	0.02	-0.07	0.14	LU+6	-0.3243	0.062	0.045	-0.039	0.086
LU+7	-0.238	0.12	-0.02	0.07	0.14	LU+7	-0.3176	-0.102	0.021	0.040	0.112
LU+8	-0.153	-0.03	-0.05	0.07	0.09	LU+8	-0.2188	-0.058	-0.140	-0.185	0.239
LU+9	-0.153	0.03	0.05	-0.07	0.09	LU+9	-0.2126	0.042	0.147	0.171	0.229
LU+10	-0.103	-0.08	-0.09	0.02	0.12	LU+10	-0.1774	-0.171	-0.048	-0.105	0.206
LU+11	-0.103	0.08	0.09	-0.02	0.12	LU+11	-0.1753	0.214	0.045	0.085	0.235
LU+12	-0.053	0.01	0.12	-0.04	0.13	LU+12	-0.1281	0.045	-0.077	-0.327	0.339
LU+13	-0.053	-0.01	-0.12	0.04	0.13	LU+13	-0.1201	-0.018	0.090	0.170	0.193
LU+14	-0.010	-0.16	0.00	-0.03	0.16	LU+14	-0.0723	-0.018	-0.086	-0.378	0.388
LU+15	-0.010	0.16	0.00	0.03	0.16	LU+15	-0.0442	-0.014	-0.009	-0.671	0.671
LU+16	0.069	0.00	-0.08	-0.01	0.08	LU+16	-0.0196	-0.002	0.060	-0.055	0.081
LU+17	0.069	0.00	0.08	0.01	0.08	LU+17	-0.0058	0.028	-0.014	-0.368	0.369
LU+18	0.107	-0.09	-0.13	-0.10	0.18	LU+18	0.0124	-0.058	0.116	-0.230	0.264
LU+19	0.107	0.09	0.13	0.10	0.18	LU+19	0.0219	0.058	-0.111	-0.065	0.141
LU+20	0.147	-0.07	0.03	0.03	0.08	LU+20	0.043	0.027	-0.003	-0.406	0.407
LU+21	0.147	0.07	-0.03	-0.03	0.08	LU+21	0.0538	0.039	-0.036	-0.216	0.222
LU+22	0.171	-0.15	0.04	0.02	0.16	LU+22	0.0775	-0.029	0.040	-0.094	0.106
LU+23	0.171	0.15	-0.04	-0.02	0.16						

SI Table S2: Table showing SKSO energy eigenvalues and magnetization projections for the pristine NC and doped NC. For the pristine NC it is seen that each energy is twice degenerate with degenerate states having anti-parallel spatial magnetization and equal magnitude. For the doped NC it is observed that each energy eigenvalue is singly degenerate. States which have >10% of charge density occupied on Mn^{2+} 3d SKSOs is highlighted.

Free Energy as Function of Mn ²⁺ Spin Configuration [eV]		
S=1/2	S=3/2	S=5/2
-5355.84	-5356.76	-5358.18

SI Table S3: Computed free energy for the *doped* NC as a function of spin multiplicity of Mn²⁺ ion.



SI Figure S2: Ground-state geometry optimized Br ligand field (pink) surrounding Mn²⁺ ion (green). Five Br ligands surround the dopant with bond lengths ranging from 2.62 to 2.73 Å and form a square pyramidal geometry. The sixth Br ligand is 3.13 Å away from the dopant and is bonded to an adjacent Pb²⁺ ion.

	Doped NC - Spin /alpha				Doped NC - Spin /beta			
	Mn(3d)	Br(4p)	Pb(6s)	Pb(6p)	Mn(3d)	Br(4p)	Pb(6s)	Pb(6p)
HO-10	0.18	0.59	0.09	0.01	0.00	0.61	0.17	0.01
HO-9	0.03	0.66	0.16	0.01	0.00	0.57	0.17	0.02
HO-8	0.02	0.75	0.11	0.01	0.00	0.59	0.17	0.01
HO-7	0.03	0.69	0.13	0.01	0.00	0.64	0.18	0.01
HO-6	0.01	0.59	0.18	0.01	0.00	0.56	0.18	0.02
HO-5	0.00	0.57	0.22	0.02	0.00	0.73	0.14	0.01
HO-4	0.01	0.54	0.21	0.01	0.00	0.73	0.13	0.01
HO-3	0.00	0.50	0.22	0.01	0.00	0.59	0.21	0.02
HO-2	0.01	0.48	0.22	0.01	0.00	0.57	0.21	0.01
HO-1	0.48	0.40	0.05	0.02	0.00	0.50	0.23	0.01
HO-0	0.54	0.40	0.02	0.01	0.00	0.49	0.23	0.01
LU+0	0.00	0.06	0.01	0.75	0.80	0.03	0.00	0.14
LU+1	0.00	0.04	0.01	0.76	0.91	0.03	0.00	0.06
LU+2	0.00	0.03	0.01	0.79	0.46	0.04	0.00	0.41
LU+3	0.00	0.04	0.01	0.77	0.94	0.03	0.00	0.03
LU+4	0.00	0.04	0.01	0.76	0.74	0.03	0.00	0.19
LU+5	0.00	0.03	0.00	0.75	0.06	0.03	0.00	0.71
LU+6	0.00	0.06	0.00	0.77	0.05	0.03	0.01	0.74
LU+7	0.00	0.07	0.00	0.76	0.05	0.04	0.01	0.74
LU+8	0.00	0.04	0.00	0.75	0.05	0.04	0.00	0.73
LU+9	0.00	0.05	0.01	0.77	0.03	0.03	0.00	0.72
LU+10	0.00	0.02	0.00	0.72	0.62	0.03	0.01	0.27

Doped NC – Spinor						
	Mn(dz2)	Mn(x2-y2)	Mn(3d)	Br(4p)	Pb(6s)	Pb(6p)
HO-10	0.00	0.00	0.02	0.68	0.15	0.00
HO-9	0.00	0.01	0.02	0.69	0.16	0.01
HO-8	0.00	0.00	0.01	0.68	0.17	0.01
HO-7	0.00	0.00	0.01	0.61	0.20	0.01
HO-6	0.00	0.00	0.00	0.58	0.21	0.01
HO-5	0.00	0.00	0.00	0.57	0.21	0.01
HO-4	0.00	0.00	0.01	0.59	0.21	0.01
HO-3	0.00	0.01	0.01	0.53	0.21	0.01
HO-2	0.00	0.00	0.00	0.54	0.22	0.01
HO-1	0.12	0.33	0.46	0.42	0.05	0.02
HO-0	0.40	0.14	0.54	0.40	0.02	0.01
LU+0	0.00	0.00	0.01	0.04	0.01	0.82
LU+1	0.00	0.00	0.00	0.05	0.01	0.82

LU+2	0.00	0.03	0.04	0.04	0.00	0.80
LU+3	0.01	0.00	0.01	0.05	0.00	0.82
LU+4	0.00	0.02	0.03	0.06	0.01	0.80
LU+5	0.00	0.00	0.01	0.05	0.01	0.82
LU+6	0.01	0.02	0.03	0.08	0.00	0.79
LU+7	0.00	0.00	0.01	0.07	0.01	0.81
LU+8	0.01	0.02	0.05	0.07	0.00	0.78
LU+9	0.00	0.00	0.01	0.06	0.01	0.82
LU+10	0.01	0.02	0.06	0.06	0.01	0.78

SI Table S4: pDOS of SKSOs near for HOMO-LUMO gap in the doped QD for SP and SKSO calculations. The only Mn^{2+} 3d states that provide significant contributions are the $3d_{z^2}$ and $3d_{x^2-y^2}$ at HO and HO-1, respectively. It is seen that these 3d states hybridize with each other and with Br 4p. The conduction band edge is primarily composed of Pb 6p for the SKSO basis. Shaded regions represent KSO densities that provide >10%.

<i>Pristine QD, Spin-Restricted</i>				<i>Pristine QD, NCS + SOC</i>			
<i>i</i>	<i>j</i>	eV	OS	<i>l</i>	<i>j</i>	eV	OS
HO	LU	3.12	6.73	HO-1	LU+1	2.38	1.15
HO-6	LU+4	3.59	5.41	HO-1	LU	2.38	0.65

HO	LU+4	3.29	5.30	HO-6	LU+11	3.09	0.47
HO-7	LU+1	3.51	4.83	HO-7	LU+11	3.09	0.43
HO-3	LU+16	3.73	4.52	HO-13	LU+2	2.90	0.36
HO-14	LU+5	3.82	3.70	HO	LU+1	2.38	0.34
HO-16	LU+5	3.85	3.47	HO-13	LU+2	2.90	0.32
HO-15	LU+11	3.94	3.24	HO-9	LU+1	2.67	0.28
HO-3	LU+13	3.70	2.88	HO-13	LU+4	2.97	0.27
HO-33	LU+2	3.98	2.79	HO-11	LU+9	3.07	0.26
HO-2	LU+1	3.43	2.71	HO-4	LU+3	2.83	0.22
HO-30	LU+2	3.96	2.67	HO-3	LU+14	3.08	0.22
HO-37	LU+2	4.01	2.60	HO	LU	2.38	0.22
HO-6	LU	3.42	2.56	HO-13	LU+5	2.97	0.21
HO-20	LU	3.68	2.45	HO-3	LU+15	3.08	0.20
<i>Doped QD, Spin α</i>				<i>Doped QD, Spin β</i>			
<i>i</i>	<i>j</i>	eV	OS	<i>l</i>	<i>j</i>	eV	OS
HO-10	LU+9	3.96	7.12	HO-11	LU+9	3.74	5.50
HO-15	LU+4	3.76	5.81	HO-1	LU+5	3.44	5.40
HO-9	LU+4	3.63	4.89	HO-8	LU+8	3.62	5.20
HO-3	LU+1	3.43	4.56	HO-18	LU+9	3.88	4.44
HO-21	LU+5	3.88	3.73	HO-6	LU+5	3.51	4.32
HO-3	LU	3.27	3.70	HO-1	LU+21	3.74	2.75
HO-26	LU+19	4.17	2.99	HO-1	LU+2	3.29	2.72
HO-4	LU+1	3.45	2.70	HO-9	LU+28	4.01	2.70
HO-2	LU+9	3.56	2.50	HO-6	LU+7	3.62	2.59
HO-3	LU+6	3.60	2.49	HO	LU+28	3.73	2.43
HO-2	LU+5	3.46	2.48	HO-1	LU+11	3.60	2.36
HO-3	LU+16	3.74	2.38	HO-2	LU+5	3.45	2.35
HO-2	LU+24	3.74	2.33	HO-13	LU+9	3.80	2.17
HO-2	LU+1	3.33	2.32	HO-4	LU+15	3.72	2.06
HO-6	LU+1	3.48	2.28	HO	LU+15	3.57	2.03

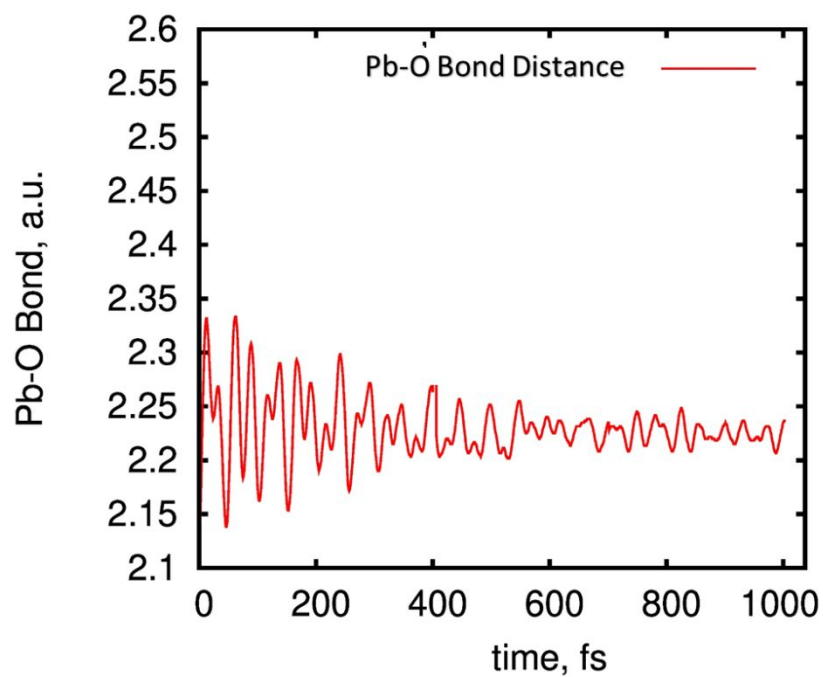
<i>Doped QD, NCS + SOC</i>			
<i>l</i>	<i>j</i>	eV	OS
HO-5	LU	2.63	0.46
HO-7	LU+3	2.80	0.46
HO-5	LU+1	2.63	0.40
HO-16	LU+5	2.93	0.32
HO-13	LU+9	3.04	0.28
HO-7	LU+6	2.88	0.26
HO-3	LU+15	2.73	0.24
HO-10	LU+9	3.02	0.22
HO-1	LU+36	3.11	0.19

HO-3	LU+13	2.97	0.19
HO-3	LU+6	2.77	0.18
HO-10	LU+6	2.67	0.18
HO-1	LU+11	2.62	0.18
HO-4	LU	2.63	0.18
HO-4	LU+1	2.63	0.18

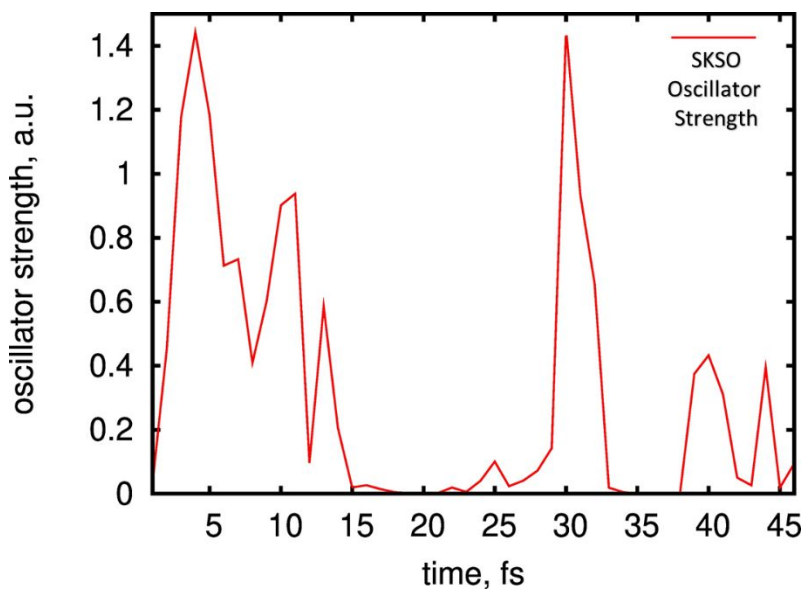
SI Table S5: Most probable excitations between pristine and doped NCs KSO/SKSO *i* and *j* with transition energy eV based on oscillator strengths.

<i>Doped QD - Spinor</i>			
Mn ²⁺ d-d transitions			
<i>i</i>	<i>j</i>	eV	OS
HO	LU+12	2.20	0.0146
HO	LU+14	2.25	0.0004
HO	LU+15	2.28	0.0020
HO	LU+16	2.31	0.0009
HO	LU+17	2.32	0.0073
HO	LU+18	2.34	0.0048
HO	LU+19	2.35	0.0024
HO	LU+20	2.37	0.0062

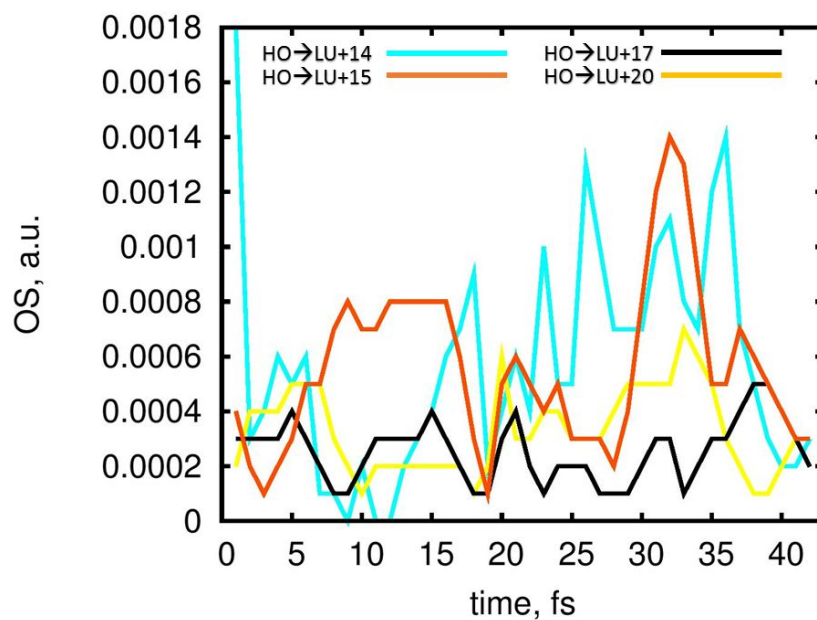
SI Table S6: Manifold of low probability d-d transitions in the doped QD which corresponds to the inset of **Figure 5(b)**.



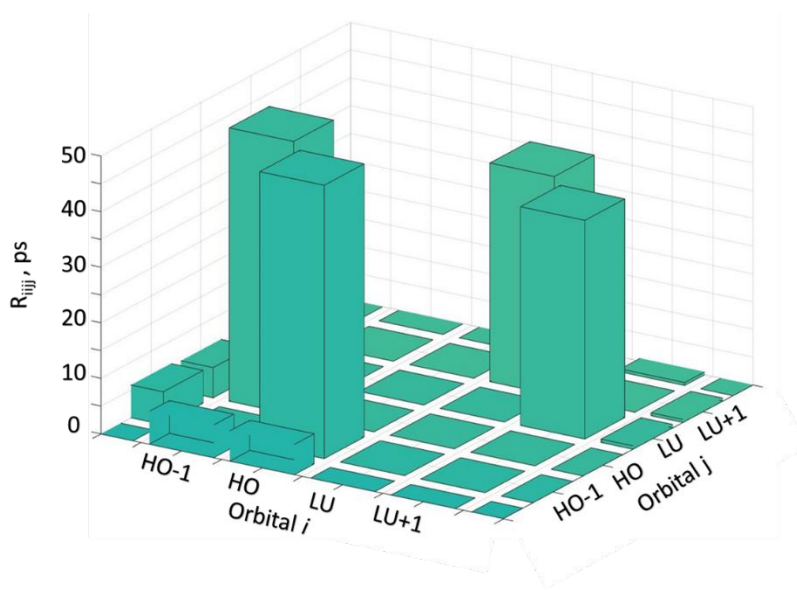
SI Figure S3: Plot of the average Pb-O bond distance computed from RDF along the adiabatic MD trajectory for the pristine NC.



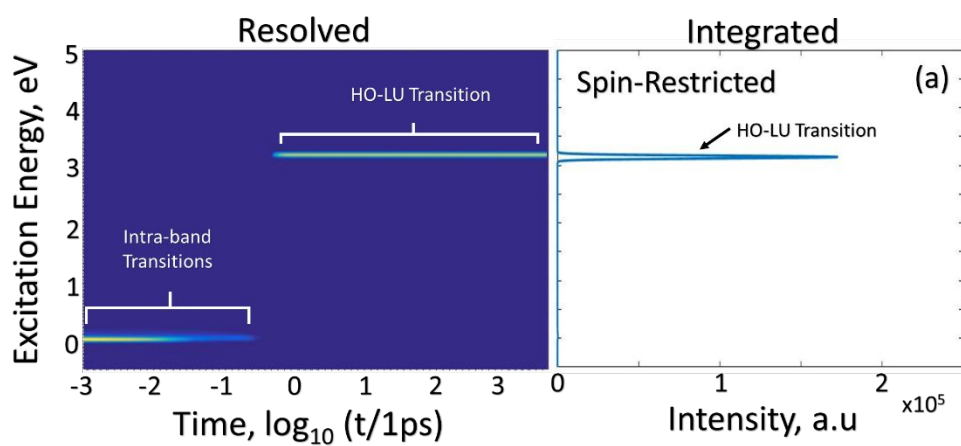
SI Figure S4: SKSO computed HO-LU oscillator strength for the pristine QD during the first 46 steps of adiabatic MD trajectory. A 'flickering' effect occurs were the QD fluctuates between bright and dark states. This is attributed to momentary surface trap state formation due to Pb-O bond fluctuations.

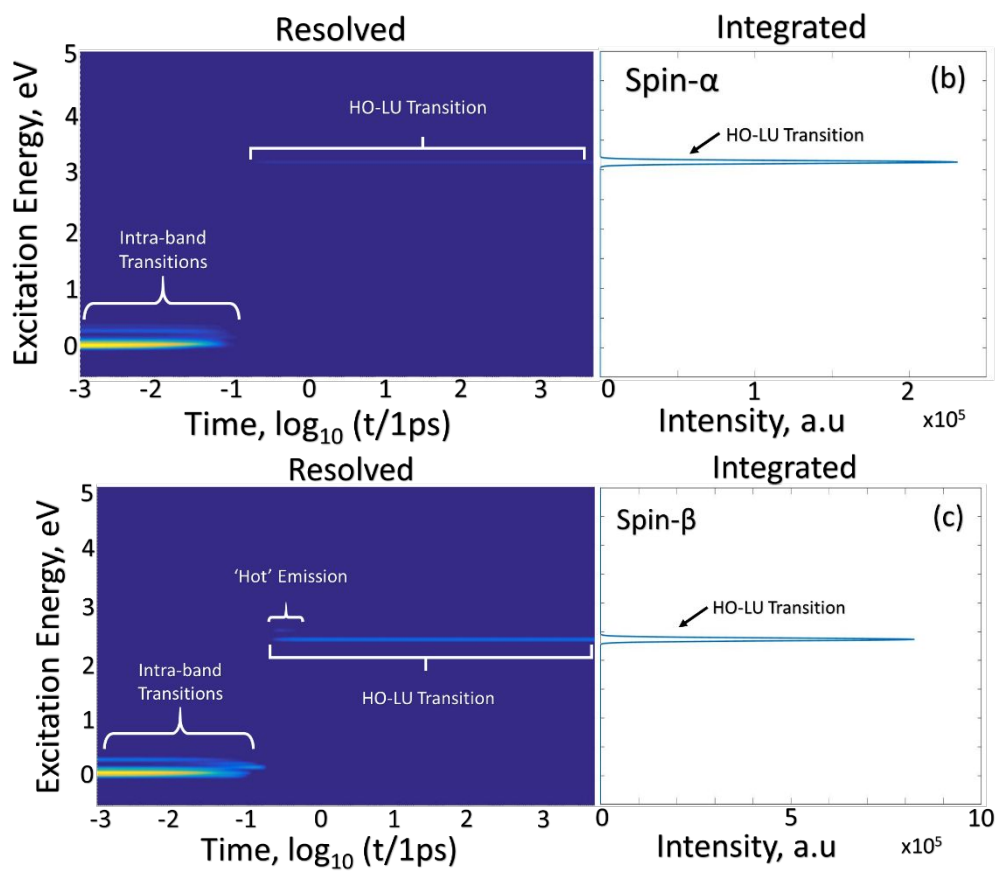


SI Figure S5: SKSO computed oscillator strength for doped QD d-d transitions during the first 43 steps of adiabatic MD trajectory.

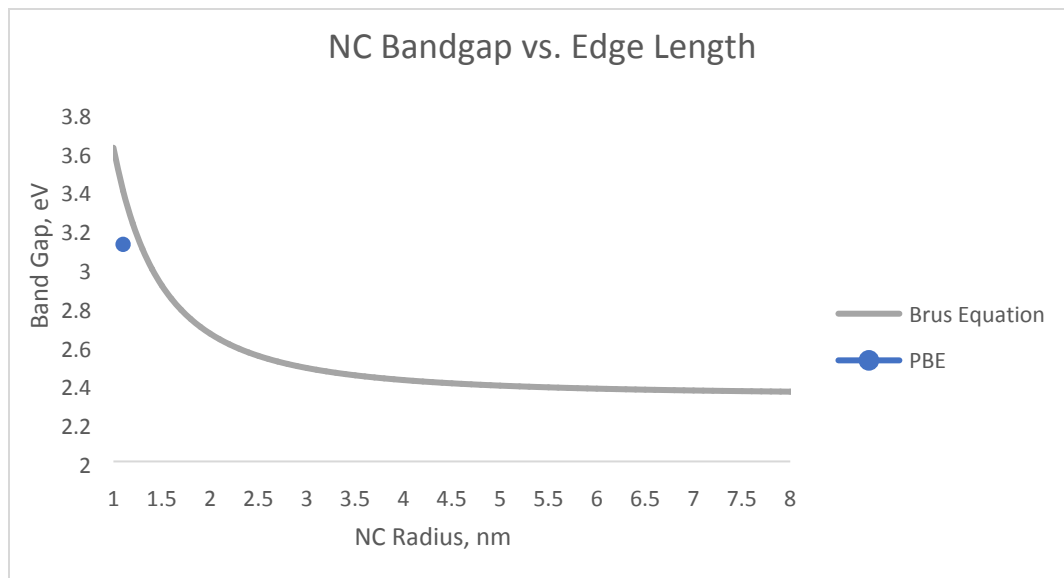


SI Figure S6: Typical Redfield tensor elements at the HO-LU transition. HO and LU have a large energy offset, which means they will have small coupling values and very slow rates of non-radiative recombination across the bandgap. The SKSO pristine and doped NC have non-radiative lifetimes of 1.18 ns and 97.8 ps, respectively.





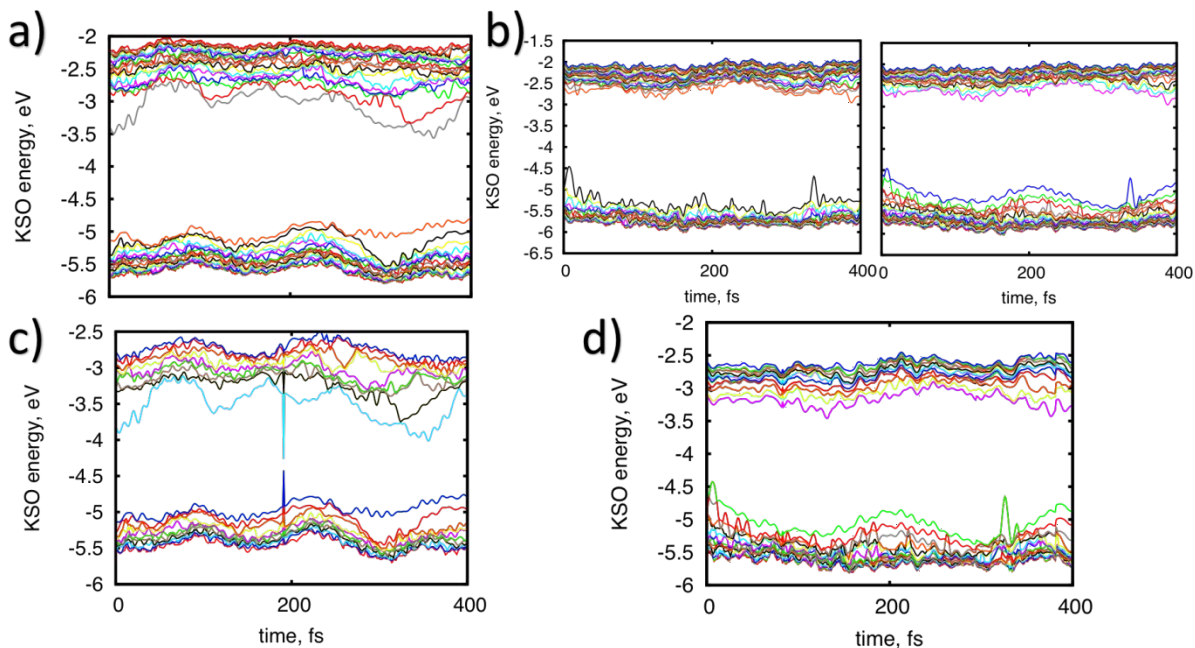
SI Figure S7: (a) SR PBE computed time resolved (left) and time integrated (right) spectra for the pristine NC. (b) spin α emission and (c) spin β emission along excited-state trajectory for the doped NC.



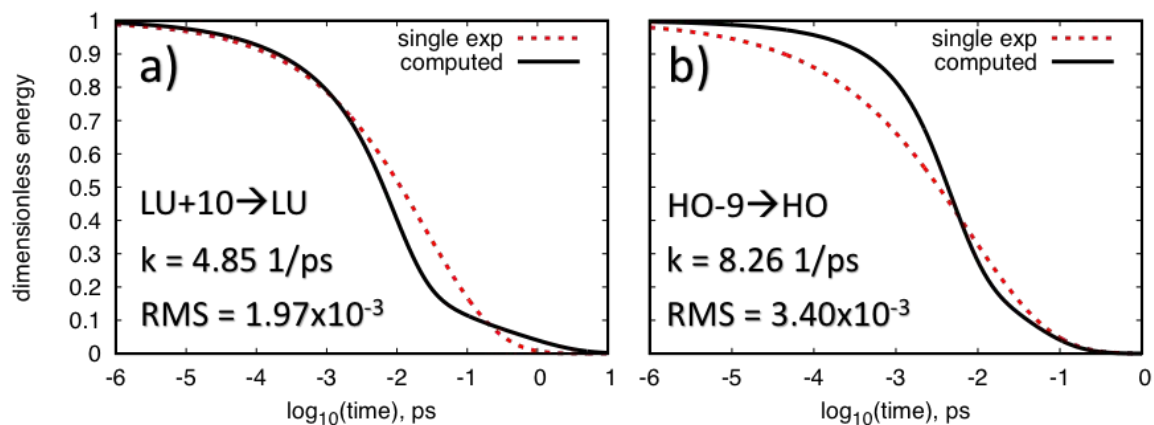
SI Figure S8: Plot of pristine CsPbBr_3 bandgap energy as a function of NC radius based on the effective mass approximation in a spherical potential $\Delta E = \frac{\hbar^2 \pi^2}{2m^* r^2}$. Effective masses of charge carriers was sourced from cited paper¹. Since the NCs are cubic in morphology the radius is approximated as center to corner distance of the NC giving a radius of $\sqrt{2} * 0.75 \text{ nm} = 1.06 \text{ nm}$. It is seen that for a NC in radius of 1.06 nm corresponds to a bandgap of 3.41 eV in the effective mass approximation. The computed bandgap of 3.12 eV in SR basis with PBE functional (blue dot) is in good agreement with quantization trend.

Model : State	ΔE_{SOC} (eV)
Intrinsic QD : HO ($\text{Pb}^{2+} 6s / \text{Br}^- 4p$)	0.083
Intrinsic QD : LU ($\text{Pb}^{2+} 6p$)	0.741
Doped QD : HO ($\text{Br}^- 4p / \text{Mn}^{2+} 3d$)	0.008
Doped QD : HO-1 ($\text{Br}^- 4p / \text{Mn}^{2+} 3d$)	0.011

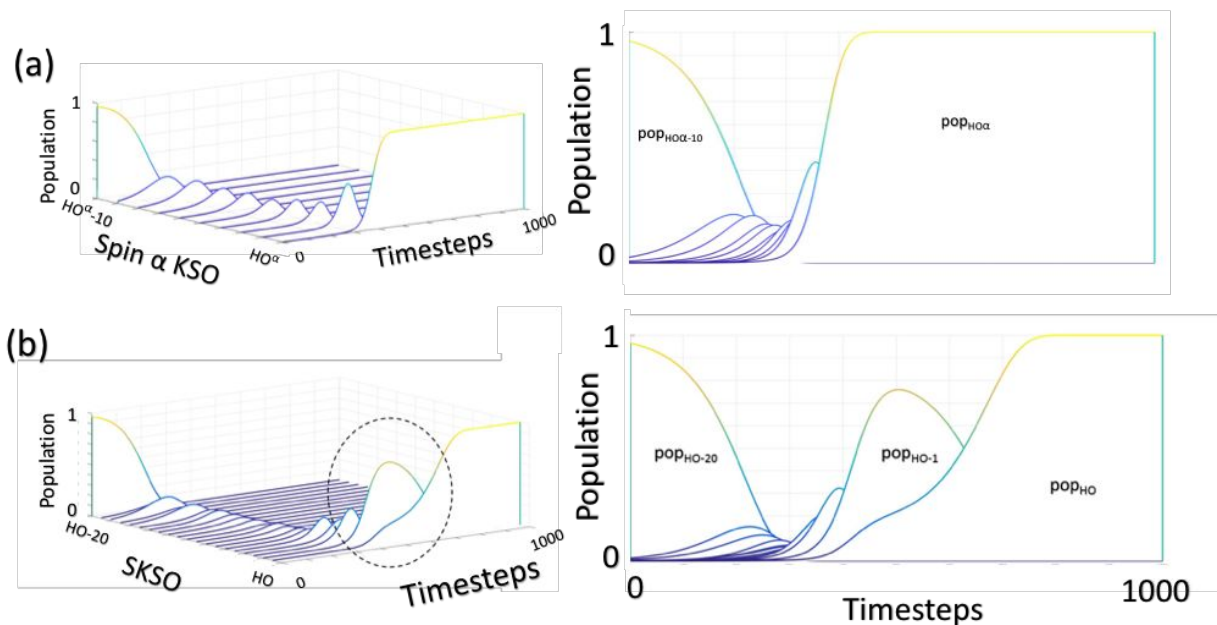
SI Table S7: Quantification of LS coupling, inferred from ΔE_{SOC} , for relevant SKSOs near the band edges. ΔE_{SOC} represents the difference in band energy comparing SR/SP KSOs and SKSOs. It is seen that the $\text{Pb}^{2+} 6p$ states in the intrinsic NC display orders of magnitude larger ΔE_{SOC} than the hybridized $\text{Pb}^{2+} 6s / \text{Br}^- 4p$ or hybridized $\text{Br}^- 4p / \text{Mn}^{2+} 3d$ states in the doped NC. These trends can be understood from 1st order perturbation theory as discussed in the text.



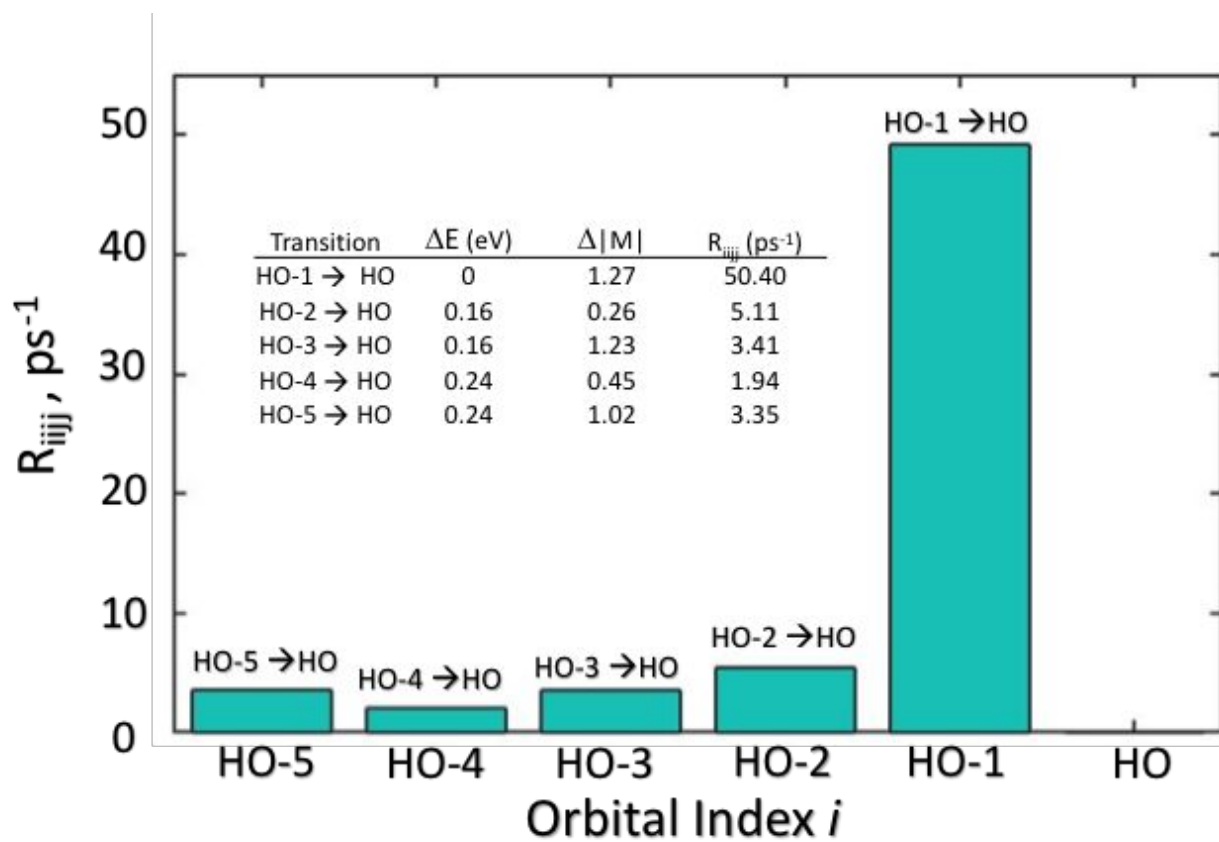
SI Figure S9: Comparing energy fluctuations for a) SR and c) SOC computed energies for the *intrinsic* NC. SI Figure zzz also shows energy fluctuations comparing b) SP and d) SOC calculations for the *doped* NC. It is seen that in the valence band there is negligible difference in energy fluctuations between SR/SP and SOC calculations. In the conduction band there are slight differences in spacing between energy states due to large SOC experienced by Pb $6p$ states which makes the DOS less dense.



SI Figure S10: Computed dimensionless energy decay curve (black, solid) and single exponential decay (red, dashed) for (a) LU+10 to LU and (b) HO-9 to HO respectively. For each panel the single exponential rate component and RMS error are shown.



SI Figure S11: Illustrating difference in non-radiative relaxation between (a) spin α and (b) SKSO basis. In both (a) and (b) a hole is initialized occupying states that have the same energy offset $\epsilon_{HO} - \epsilon_x = 1.03$ eV and is allowed to relax to the HO state. It is seen that near HO rates of relaxation are slower in the SKSO basis as population accumulates between HO-2 and HO-1. The corresponding relaxation rates for spin α and SKSO relaxation are 4.46 and 0.08 1/ps, respectively.



SI Figure S12: Projection of Redfield Tensor for *pristine* NC along $R_{HO,HO-x}$ axis where $x=1,2,3,4,5$. The inset table refers shows transition energy ΔE , change in magnetization $\Delta|M|$, and Redfield tensor elements R_{ijkl} . It is noted that each eigenenergy is two-fold degenerate. Degenerate bands have anti-parallel projections of magnetization components. This leads to state-to-state transitions that have same energies, but different magnetization.

1. Protesescu, L.; Yakunin, S.; Bodnarchuk, M. I.; Krieg, F.; Caputo, R.; Hendon, C. H.; Yang, R. X.; Walsh, A.; Kovalenko, M. V., Nanocrystals of cesium lead halide perovskites (CsPbX₃, x = Cl, Br, and I): Novel optoelectronic materials showing bright emission with wide color gamut. *Nano Lett* **2015**, *15* (6), 3692-6.